JAMA Ophthalmology | Original Investigation

Progression of Photoreceptor Degeneration in Geographic Atrophy Secondary to Age-related Macular Degeneration

Maximilian Pfau, MD; Leon von der Emde; Luis de Sisternes, PhD; Joelle A. Hallak, PhD; Theodore Leng, MD; Steffen Schmitz-Valckenberg, MD; Frank G. Holz, MD; Monika Fleckenstein, MD; Daniel L. Rubin, MD, MS

IMPORTANCE Sensitive outcome measures for disease progression are needed for treatment trials in geographic atrophy (GA) secondary to age-related macular degeneration (AMD).

OBJECTIVE To quantify photoreceptor degeneration outside regions of GA in eyes with nonexudative AMD, to evaluate its association with future GA progression, and to characterize its spatio-temporal progression.

DESIGN, SETTING, AND PARTICIPANTS Monocenter cohort study (Directional Spread in Geographic Atrophy [NCT02051998]) and analysis of data from a normative data study at a tertiary referral center. One hundred fifty-eight eyes of 89 patients with a mean (SD) age of 77.7 (7.1) years, median area of GA of 8.87 mm^2 (IQR, 4.09-15.60), and median follow-up of 1.1 years (IQR, 0.52-1.7 years), as well as 93 normal eyes from 93 participants.

EXPOSURES Longitudinal spectral-domain optical coherence tomography (SD-OCT) volume scans (121 B-scans across 30° × 25°) were segmented with a deep-learning pipeline and standardized in a pointwise manner with age-adjusted normal data (*z* scores). Outer nuclear layer (ONL), photoreceptor inner segment (IS), and outer segment (OS) thickness were quantified along evenly spaced contour lines surrounding GA lesions. Linear mixed models were applied to assess the association between photoreceptor-related imaging features and GA progression rates and characterize the pattern of photoreceptor degeneration over time.

MAIN OUTCOMES AND MEASURES Association of ONL thinning with follow-up time (after adjusting for age, retinal topography [*z* score], and distance to the GA boundary).

RESULTS The study included 158 eyes of 89 patients (51 women and 38 men) with a mean (SD) age of 77.7 (7.1) years. The fully automated B-scan segmentation was accurate (dice coefficient, 0.82; 95% CI, 0.80-0.85; compared with manual markings) and revealed a marked interpatient variability in photoreceptor degeneration. The ellipsoid zone (EZ) loss-to-GA boundary distance and OS thickness were prognostic for future progression rates. Outer nuclear layer and IS thinning over time was significant even when adjusting for age and proximity to the GA boundary (estimates of −0.16 µm/y; 95% CI, −0.30 to −0.02; and −0.17 µm/y; 95% CI, −0.26 to −0.09).

CONCLUSIONS AND RELEVANCE Distinct and progressive alterations of photoreceptor laminae (exceeding GA spatially) were detectable and quantifiable. The degree of photoreceptor degeneration outside of regions of retinal pigment epithelium atrophy varied markedly between eyes and was associated with future GA progression. Macula-wide photoreceptor laminae thinning represents a potential candidate end point to monitor treatment effects beyond mere GA lesion size progression.

JAMA Ophthalmol. doi:10.1001/jamaophthalmol.2020.2914
Published online August 13, 2020.

Supplemental content

Author Affiliations: Department of Biomedical Data Science, Stanford University, Stanford, California (Pfau, Rubin); Department of Ophthalmology, University of Bonn, Bonn, Germany (Pfau, von der Emde, Schmitz-Valckenberg, Holz, Fleckenstein); Research and Development, Carl Zeiss Meditec Inc, Dublin, California (de Sisternes); Department of Ophthalmology and Visual Sciences, University of Illinois at Chicago (Hallak); Byers Eye Institute at Stanford, Stanford University School of Medicine, Palo Alto, California (Leng); John A. Moran Eye Center, University of Utah, Salt Lake City (Schmitz-Valckenberg, Fleckenstein).

Corresponding Author: Daniel L. Rubin, MD, MS, Stanford University, Medical School Office Building (MSOB), 1265 Welch Rd, Room X-335, MC 5464, Stanford, CA 94305-5479 (dlrubin@stanford.edu).

Age-related macular degeneration (AMD) is the leading cause of legal blindness in industrialized countries.[1-3] While anti-VEGF therapy may halt or significantly delay exudation-related vision loss in eyes with neovascular AMD,[4] no treatment is available to slow the progression of geographic atrophy (GA), the atrophic late-stage manifestation of this disease. Geographic atrophy is characterized by foci of retinal pigment epithelium (RPE) atrophy that slowly progress and merge over time, leading to corresponding visual function loss[5] that severely affects activities of daily living[6] and quality of life.[7,8]

While a lack of biological efficacy may be responsible for the negative results in large-scale therapeutic trials for GA,[9] the primary end point (change in lesion size of RPE atrophy) may have obscured potentially beneficial treatment effects unrelated to short-term RPE atrophy progression in the junctional zone. This is especially likely in the context of subretinal drusenoid deposits (SDD, or reticular pseudodrusen), where progressive photoreceptor degeneration with persistent RPE has been described based on spectral-domain optical coherence tomography (SD-OCT) imaging as well as histopathology.[10-12] In the setting of intermediate AMD, multiple quantitative imaging features have been proposed to quantify this type of outer retinal degeneration, including outer nuclear layer (ONL), photoreceptor inner segment (IS), and outer segment (OS) thickness as well as the ellipsoid zone (EZ) reflectivity.[12-14] Similarly, photoreceptor loss has been evidenced in the context of neovascular AMD including regions outside macular atrophy.[15] In terms of concurrent validity, these imaging features of outer retinal degeneration were shown to be strongly associated with loss of mesopic and scotopic light sensitivity.[12-14,16]

To date, no applicable strategy has been brought forward to quantify photoreceptor degeneration in eyes with GA, despite an international consensus terminology that introduced the term *incomplete RPE and outer retinal atrophy*.[17] Monitoring of photoreceptor degeneration over time outside of the junctional zone of GA would likely provide information not reflected by the end point RPE atrophy progression. Further, quantifying these alterations would provide the opportunity to probe therapeutic interventions targeting photoreceptor degeneration initially in patients with GA that present with a favorable benefit-risk trade-off compared with patients with intermediate AMD. Accordingly, the spatial distribution of photoreceptor degeneration (in terms of distance to the RPE atrophy boundary) in eyes with GA secondary to AMD, and its potential progression over time, warrants further investigation.

Using longitudinal natural-history data, we, for the first time to our knowledge, (1) assessed the accuracy of a deep-learning (DL)–based image segmentation and quantification model to extract biomarkers of ONL, OS, and IS thinning in eyes with GA (reliability) and (2) quantified the magnitude of photoreceptor degeneration outside of GA and its association with future GA progression (predictive validity). Lastly, we (3) provided a spatiotemporal model for photoreceptor degeneration as a function of a junctional-zone component and a distinct macula-wide component, underscoring the ability to detect change of the latter.

Key Points

Question Is progressive photoreceptor degeneration outside of geographic atrophy (GA) in eyes with nonexudative age-related macular degeneration evident and quantifiable?

Findings In this cohort study, fully automated segmentation facilitated an accurate quantification of photoreceptor degeneration. Progressive degeneration of the outer nuclear layer and photoreceptor inner segments was evident, even accounting for age or distance to the GA boundary.

Meaning Progressive alterations of photoreceptor laminae (exceeding GA spatially) were detectable and quantifiable. These findings support macula-wide photoreceptor degeneration as a candidate end point to monitor treatment effects beyond GA progression.

Methods

Patients

Patients included in this analysis participated in the noninterventional, prospective, longitudinal natural history Directional Spread in Geographic Atrophy 2 study.[18-20] This study conducted at the Department of Ophthalmology, University of Bonn, Germany, adhered to the tenets of the Declaration of Helsinki, and was approved by the institutional review board (institutional review board of the University of Bonn). Written informed consent was obtained from all participants. No compensation/incentive was offered to the participants. The inclusion criteria have been described previously in detail.[18,19] Briefly, patients needed to be older than 55 years at the time of inclusion and had to exhibit GA secondary to AMD in at least 1 eye.[21] The diagnosis of AMD was based on the presence of drusen and hyperpigmentary changes and a compatible fundus autofluorescence (FAF) phenotype, while excluding FAF phenotypes of mimicking diseases such as late-onset Stargardt disease.[22] Exclusion criteria were any history of vitreoretinal surgery, laser photocoagulation, and radiation therapy or other retinal diseases in the study eye such as diabetic retinopathy.[21] Patients were seen for up to 24 months at 6-month or 12-month intervals, respectively. For the analysis in this study, eyes with any clinical evidence of nonexudative type 1 choroidal neovascularization were excluded.[20] Imaging data for control eyes were obtained from patients' companions and hospital patients with a healthy fellow eye (ethics approval ID: 191/16).

Imaging Protocol

Following pupil dilatation with tropicamide, 0.5%, and phenylephrine, 2.5%, patients underwent (among other investigations) 30° × 30° FAF imaging (λ excitation, 488 nm; λ emission, 500-700 nm), 30° × 30° infrared reflectance (λ 815 nm) imaging, and 30° × 25° SD-OCT imaging (121 B-scans, ART 25) using a Spectralis HRA+OCT2 (Heidelberg Engineering).

Deep-Learning–Based Image Segmentation

For the SD-OCT B-scan multilayer segmentation (**Figure 1**), the same layer definitions were applied for the inner retina, ONL,

Figure 1. Image Segmentation Pipeline

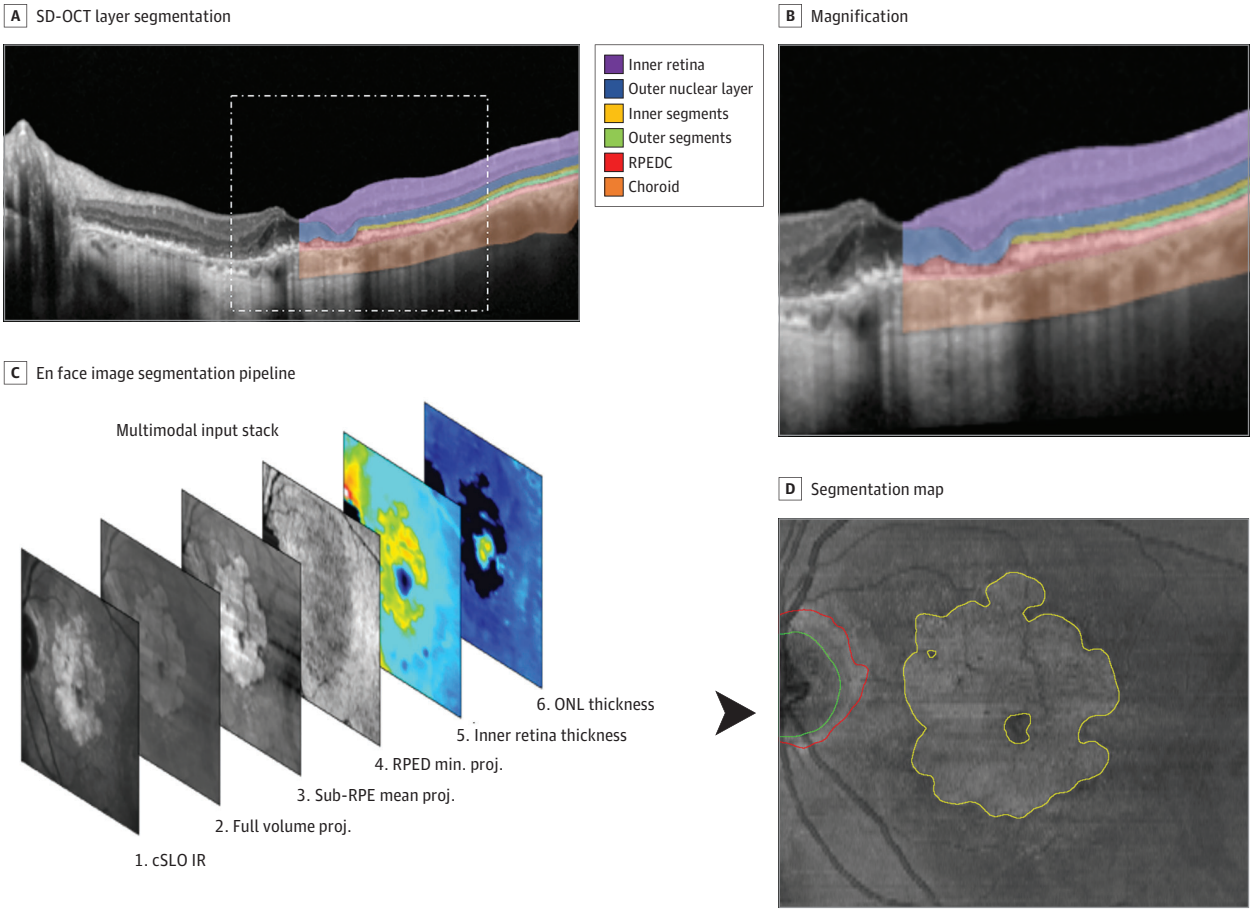

A, Resulting segmentation generated by the first convolutional neural network (CNN, Deeplabv3 model with a ResNet-50 backbone) providing a 6-layer segmentation: inner retina, outer nuclear layer (ONL), photoreceptor inner and outer segments, retinal pigment epithelium drusen complex (RPEDC, including reticular pseudodrusen, retinal pigment epithelium (RPE), drusen, and basal laminar deposit, and choroid. The insert on the upper right side provides a magnified view (B). En face projections and thickness maps generated based on these segmentations as well as the confocal laser scanning laser ophthalmoscopy (cSLO) infrared reflection (IR) image were passed on as 6-layered input stack to the second CNN (Deeplabv3 model with a ResNet-50 backbone). As shown in D, the second CNN provided an en face segmentation of geographic atrophy (yellow outline), peripapillary atrophy (red outline), and the optic nerve head (green outline). proj. indicates projection, SD-OCT, spectral-domain optical coherence tomography.

IS, OS, and RPE drusen complex (RPEDC) as in previous studies.[16,23] Henle fiber layer and hyporeflective wedge-shaped bands were counted toward the ONL; the RPEDC comprised reticular pseudodrusen, RPE, and drusen as well as basal laminar deposit in this study (Figure 1). This combined grading of subretinal and subRPE deposits was elected in consideration of the interrater variability and severe alterations of the retinal microstructure in eyes with GA. For this as well as the en face segmentation task of GA and peripapillary atrophy, completely separate (patientwise splits) training, validation, and testing data were available for training of a convolutional neural network (eMethods in the Supplement).

Segmentation and Standardization of Imaging Data

After validation of the image segmentation workflow, all images were segmented using the previously described pipeline (Figure 1). This was followed by standardization of all data (conversion to *z* scores) based on age-based and location-adjusted normative data (**Figure 2**; eMethods in the Supplement).

Feature Extraction

The extraction of imaging features was performed in 2 principal ways (eMethods in the Supplement). First, the median EZ-loss-to-GA boundary distance and ELM-descent-to-GA boundary distance were extracted (negative values indicating a boundary position within GA and positive values outside of GA). Second, along evenly spaced contour lines around the lesion of GA (width, approximately 0.43° [approximately 126 µm]), the mean thickness for the inner retina, ONL, IS, OS, RPEDC, and choroid were extracted (eFigure 1 in the Supplement).

Statistical Analyses

Statistical analyses were performed in the software environment R using the add-on packages lme4 and glmmLasso.[24,25]

Figure 2. Spatial Registration and Data Standardization

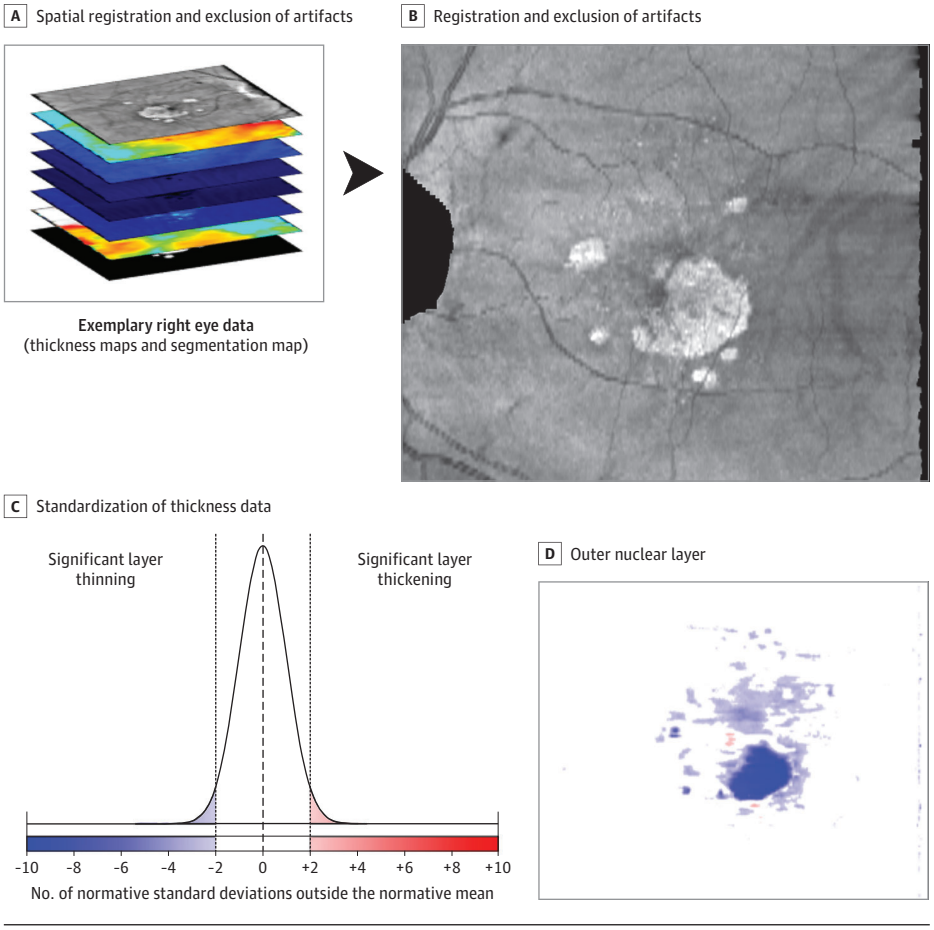

As a first step (A), all eyes were registered to a left-eye reference coordinate system followed by exclusion of (1) the optic nerve head or peripapillary atrophy, (2) vignetting artifacts, or (3) regions with lack of normative data (peripapillary retina). Next (B), each pointwise thickness value was standardized (*z* score, accounting for retinal location and age). For clarity, nonsignificant alterations in thickness (−2 to 2 normative SDs) were plotted with the same color.

Cohort estimates for the annual absolute and square-root-transformed progression rates were obtained using linear mixed models with eyes nested in patients as random-effects term.

The dice similarity coefficient was used to assess the test-set segmentation accuracies. Linear mixed models (considering B-scans nested in patients as random-effects term) were applied to determine the association of the reader-pairing (reader 1 vs reader 2, reader 1 vs DL, and reader 2 vs DL) and the annotated layer/structure as fixed effects, with the dice similarity coefficient as dependent variable.

Cross-validated LASSO regression was applied to investigate the prognostic value of these imaging features for GA progression with a parsimonious, interpretable linear model (eMethods in the Supplement).

To analyze whether the degree of outer retina retinal degeneration was only associated with the distance of GA boundary (junctional zone component) or whether an additional macula-wide component of degeneration over time was evident, mixed-linear models were applied. For the null model, ONL, IS, or OS thicknesses served as dependent variables, distance to the GA boundary as an independent variable, and eyes nested in patients were considered as a random-effects term. Likelihood ratio tests were applied to examine whether follow-up time (as macula-wide variable) exhibited an additional independent association with the layer thicknesses.

Results

Cohort

A total of 158 eyes with GA secondary to AMD from 89 patients (51 female and 38 male) were included in this analysis. The mean (SD) age at baseline was 77.7 (7.1) years (range, 64.1-93.7 years). The median follow-up time was 1.1 years (IQR, 0.52-1.7) corresponding to a median of 2 follow-up visits (IQR, 1-4). The median area of GA in patients was 8.87 mm^2 (IQR, 4.09-15.60). Patients exhibited on average an annual absolute GA progression rate of 1.59 mm^2/y (95% CI, 1.46-1.71), corresponding to a square-root-transformed GA progression rate of 0.26 mm/y (95% CI, 0.24-0.27). Further, 93 normal eyes from 93 patients (age range, 18.0-84.5 years) were included for standardization of patient data.

Accuracy of Automated Quantification of Retinal Layers

The average dice similarity coefficient as a measure of overlap between human reader 1 and 2 and the automated segmentation was overall good for the test set (estimate, 0.82;

Figure 3. Exemplary Patients

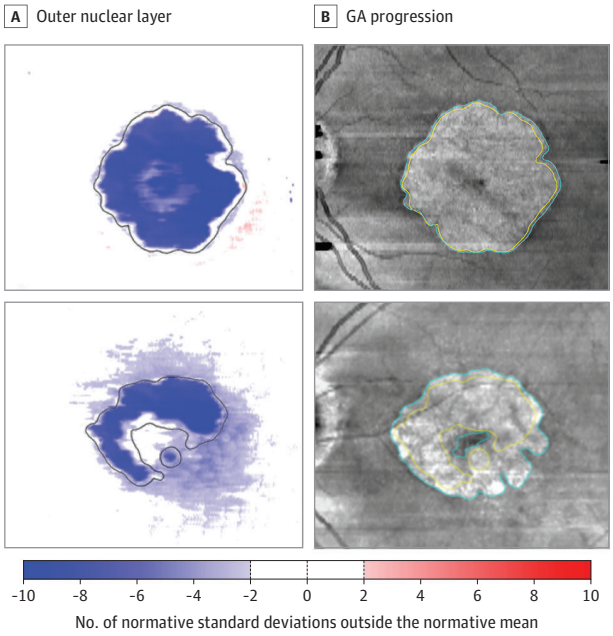

A, Standardized (*z* scores, accounting for retinal location and age) outer nuclear layer thickness maps of 2 patients. The area of retinal pigment epithelium atrophy is indicated by the black outline in the thickness maps. B, En face spectral-domain optical coherence tomography mean volume projections of the same patients 1 year later. The yellow and cyan outline demarcate the baseline and year 1 geographic atrophy (GA) boundaries, respectively. Notably, the first patient exhibits a milder degree of outer retinal degeneration at baseline and slower GA progression compared with the second patient. eFigure 4 in the Supplement provides a more comprehensive overview of these patients including the other outer retinal layer thicknesses.

95% CI, 0.80-0.85). The dice similarity coefficient varied in dependence of the segmented layer ($P < .001$; eFigure 2 in the Supplement) and the reader/algorithm pairing ($P < .001$). Post hoc comparison revealed that the overlap between the automated segmentation and reader 1 as well as the overlap between automated segmentation and reader 2 were both minimally, yet significantly better than the overlap between the human readers (estimate [SE], 0.039 [0.007] for DL and reader 1 vs reader 1 and reader 2; 0.02 [0.007] for DL and reader 2 vs reader 1 and reader 2). Similarly, the overall overlap for the en face segmentation between reader 1, reader 2, and the automated segmentation was excellent (0.88; 95% CI, 0.85-0.91; eFigure 3 in the Supplement). It did not vary significantly in dependence of the reader/algorithm pairing but did in dependence of the labeled structure ($P < .001$). The overlap was excellent for GA (0.96; 95% CI, 0.91-1.00) and good for the optic nerve head and peripapillary atrophy (0.88; 95% CI, 0.84-0.93 and 0.71; 95% CI, 0.66-0.75, respectively).

Photoreceptor Degeneration in Eyes With GA

Photoreceptor degeneration could be mostly limited to the area of GA or exceed the boundaries of GA both locally and globally (first and second patient in **Figure 3**; eFigure 4 in the Supplement). Quantitatively, the median ELM-decent-to-GA boundary distance was −11.45 µm (IQR, −29.75 to 48.09; negative sign indicating a position internal to the GA boundary) and the median EZ-loss-to-GA boundary distance 365.0 µm (IQR, 201.4-603.0 µm). For all photoreceptor-related layers, the degree of layer thinning varied markedly in dependence of the distance to the GA boundary. Hereby, the degree of between-eye variability was markedly higher for the OS thickness compared with ONL and IS thickness (**Figure 4**). No marked thinning or thickening could be observed in most eyes for the inner retina (eFigure 7 in the Supplement). The RPEDC was thickened toward the boundary of GA and the choroid tended to be thinner than average in most eyes (eFigure 7 in the Supplement).

Prognostic Value of Photoreceptor Degeneration for GA Progression

Qualitatively, photoreceptor degeneration outside of GA appeared to correlate with future GA progression rates (Figure 3; eFigure 4 in the Supplement). Univariate linear mixed models confirmed this observation, revealing that the EZ-loss-to-GA boundary distance and the normalized thicknesses of the ONL, OS, and IS (at various distances to the GA boundary) were all significantly associated with the future GA progression rates (**Table**). A parsimonious multivariate linear model allowed prediction of square-root-transformed GA progression rates with a mean absolute error accuracy of 0.17 mm/y, corresponding to an R^2 value (while accounting of the hierarchical structure of the data) of 0.125 (eFigure 5 in the Supplement).

Longitudinal Progression Photoreceptor Degeneration Outside of GA

Profiles for all 3 photoreceptor layer thicknesses revealed an obvious association with the distance to the GA boundary with marked thinning toward the GA boundary (junctional-zone component of outer retinal degeneration; Figure 4; eFigure 6 in the Supplement). This could be confirmed by mixed models considering the distance to the GA boundary as a fixed effect (eTable 1 in the Supplement). Although standardization of measurements in patients accounted for age on a per visit basis, addition of follow-up time as a fixed effect (macula-wide component) resulted for all 3 photoreceptor layer models in a significantly better goodness of fit (likelihood ratio tests; $P < .001$ for ONL thickness, $P < .001$ for IS thickness, and $P = .01$ for OS thickness model in eTable 1 in the Supplement). In patients, ONL thickness decreased in a macula-wide manner by an average of −0.03 normal SD/y (95% CI, −0.05 to −0.01), corresponding to approximately −0.16 µm/y; IS thickness by −0.17 normal SD/y (95% CI, −0.17 to −0.06); approximately −0.18 µm/y; and OS by −0.04 normal SD/y (95% CI, −0.10 to −0.01); approximately −0.03 µm/y. eTable 2 in the Supplement provides the estimates for models based on thickness deviation (in micrometers).

Discussion

This study outlines a fully automated image segmentation and analysis pipeline to simultaneously quantify GA progression

Figure 4. Photoreceptor Degeneration at the Boundary of Geographic Atrophy (GA)

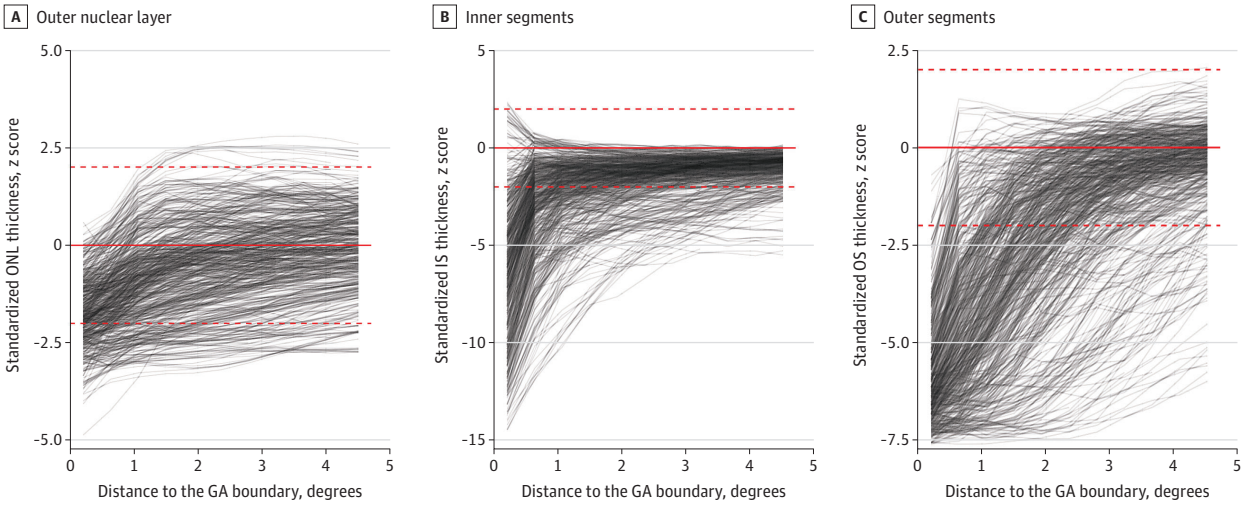

The 3 panels show the outer nuclear layer (ONL; A), photoreceptor inner segments (IS; B), and outer segments (OS; C) thicknesses in dependence of the distance to the GA boundary. The y-axis denotes the *z* scores (accounting for retinal location and age). Each visit of each eye is plotted by a semitransparent line. The red dashed lines indicate the *z* score range of −2 to 2 normative SDs. eFigure 6 in the Supplement shows these data in terms of the absolute thickness deviations.

and photoreceptor degeneration in AMD. The results indicate that imaging biomarkers of photoreceptor degeneration are associated with future GA progression rates. Further, a junctional zone component of photoreceptor degeneration relating to the distance from the GA boundary and a distinct macula-wide component of photoreceptor degeneration could be quantified independently.

Regarding GA quantification, other semiautomated quantification methods, such as the RegionFinder software (Heidelberg Engineering) for fundus autofluorescence images, have been previously validated and applied as primary end points in large clinical trials.[9,26,27] In comparison, the fully automated, multimodal deep-learning pipeline based on coacquired SD-OCT and IR images presented in this study overall reached a similar accuracy compared with semiautomated RegionFinder software annotations.[26,27] In addition, it allowed for precise retinal layer segmentation with similar accuracy to other conventional and deep-learning approaches.[28-31] Importantly, the comparison of human expert interreader variability with human vs DL variability underscores the accuracy of the GA and retinal layer segmentations.

Our proposed metrics of photoreceptor degeneration may be helpful in future clinical trials in patients with GA as an additional biomarker for patient selection/stratification or even as a structural, objective clinical end point. Previously, imaging features related to lesion shape (lesion size, lobularity, and focality),[19,32,33] RPE-associated characteristics (FAF patterns),[32] junctional-zone configuration in SD-OCT,[34] and optical coherence tomography angiography (OCTA)–based choriocapillaris flow-signal voids[35,36] were shown to be prognostic for atrophy progression. Moreover, a qualitative study by Nunes et al,[37] based on a en face projection centered to the EZ, suggested an association of photoreceptor degeneration with future atrophy progression. In this study, we now confirmed quantitatively the association of the OS thickness and EZ integrity with future GA progression rates. Concerning biologic plausibility, the observed OS thinning may be considered, (to a large extent) based on our applied layer definitions, as a sign of SDD. In AMD, SDDs were shown to be associated with high-risk genotypes,[38] impaired rod-mediated dark adaptation,[39] and increased risk for conversion from intermediate to late AMD.[40] However, the variable life-cycle trajectories of SDD, which include SDD regression, make precise quantification of SDD load challenging.[10,41] Accordingly, OS thinning, even if considered as a secondary downstream alteration to SDD, may constitute a more reliable biomarker for quantification. Of note, EZ reflectivity restoration (but in conjunction with retinal thinning) has been described following regression of SDD.[41]

In addition to application of photoreceptor degeneration imaging features as prognostic biomarkers, these features may be attractive as clinical end points. In addition to the accuracy and prognostic validity (see previous sections), concurrent validity for these features has been underscored by multiple structure-function correlation studies in intermediate AMD and GA.[12,14,42-44] Specifically, using mesopic and scotopic fundus-controlled perimetry (also termed microperimetry), it has been established for intermediate and late AMD that ONL thinning, IS thinning, and OS thinning as well as loss of the EZ are indicative of cone and rod photoreceptor dysfunction.[12,14,16,42,43] Our approach of standardizing all measurements for age on a per visit basis and using linear mixed models to adjust for the (marked) association of photoreceptor degeneration and distance to the GA boundary (junctional-zone component) allows us to quantify the distinct macula-wide component as a function of time. Conceptually analogous, a macula-wide component of dysfunction that increases with disease severity between intermediate and late AMD was ob-

Table. Univariate Association With Future (Square-Root-Transformed) Geographic Atrophy Progression Rates

Feature	Estimate, (95% CI), mm/y per feature unit	*P* value
Median EZ-loss-to-GA boundary distance, mm	0.17 (0.06 to 0.29)	.004
Median ELM-descent-to-GA boundary distance, mm	0.05 (−0.12 to 0.22)	.54
Inner retinal thickness (as *z* score)		
Contour line		
0.21° (62 µm)	0.02 (−0.02 to 0.06)	.40
1.50° (440 µm)	0.01 (−0.04 to 0.06)	.60
3.22° (944 µm)	0.01 (−0.04 to 0.06)	.62
Outer nuclear layer thickness (as *z* score)		
Contour line		
0.21° (62 µm)	−0.05 (−0.09 to 0.00)	.07
1.50° (440 µm)	−0.05 (−0.09 to 0.01)	.009
3.22° (944 µm)	−0.05 (−0.09 to 0.01)	.01
Inner segment thickness (as *z* score)		
Contour line		
0.21° (62 µm)	−0.02 (−0.03 to 0.01)	<.001
1.50° (440 µm)	−0.03 (−0.05 to 0.00)	.04
3.22° (944 µm)	−0.05 (−0.09 to 0.00)	.03
Outer segment thickness (as *z* score)		
Contour line		
0.21° (62 µm)	−0.05 (−0.09 to 0.02)	.003
1.50° (440 µm)	−0.05 (−0.07 to 0.03)	<.001
3.22° (944 µm)	−0.05 (−0.07 to 0.02)	<.001
RPEDC thickness (as *z* score)		
Contour line		
0.21° (62 µm)	0.01 (−0.00 to 0.02)	.10
1.50° (440 µm)	0.02 (0.00 to 0.04)	.01
3.22° (944 µm)	0.04 (0.02 to 0.06)	<.001
Choroidal thickness (as *z* score)		
Contour line		
0.21° (62 µm)	−0.06 (−0.11 to 0.01)	.02
1.50° (440 µm)	−0.06 (−0.12 to 0.01)	.02
3.22° (944 µm)	−0.06 (−0.12 to 0.01)	.017

Abbreviations: EZ, ellipsoid zone; RPEDC, retinal pigment epithelium drusen complex.

served for rod-mediated dark adaptation and discussed in the context of a recent OCTA study for GA.[45,46]

Regarding the other layers, the thickening of RPEDC toward the boundary of GA is very much compatible with the histopathologic description of an increased basal laminar deposit thickness[47] and stacking of RPE cells in proximity to the GA boundary.[48,49] Similarly, choroidal thinning toward the atrophy boundary is compatible with the histopathologic descriptions of choriocapillaris breakdown in the junctional zone of GA.[48]

Limitations

Various prognostic imaging features have been described for GA progression. A multimodal comparison in conjunction with feature selection is needed to identify the key prognostic features of GA progression, ideally in a spatially resolved manner.[20,50] Moreover, this study does not provide data regarding the functional implications of observed progressive photoreceptor degeneration. However, this has been addressed previously.[12,14,42-44] Axial length measurements were not available for this analysis. The presented values constitute most likely conservative estimates because refined standardization with axial length would have reduced the normative variability and consequently increased the *z* score values. While the ability to detect change for macula-wide photoreceptor degeneration was demonstrated, the signal-to-noise ratio for ONL, IS, and OS thinning over time could be improved using upcoming ultrahigh-resolution OCT technology, providing greater axial resolution.[51] This would also enhance the ability to distinguish between subretinal and sub-RPE deposits in a refined manner.[52] While the ELM descent is closely associated with the histopathologic description of GA, the loss of the EZ band and OS layer in SD-OCT spatially exceed the loss of the corresponding structures in histopathology.[47] Likely, the studied EZ and OS derived metrics for photoreceptor degeneration are a composite measure of (irreversible) atrophic changes and (potentially reversible) waveguiding alterations.[41] Notable strengths of this study include the large sample size, application of a state-of-the-art convolutional neural network for the segmentation tasks, rigorous validation of the segmentation accuracy with comparison to human interreader variability, and accurate standardization for age and retinal position. Moreover, the imaging device used in this study has been previously used in large, multicenter interventional trials (eg, NCT02247531, NCT02247479, and NCT02087085). Considering that GA progression reflects only partially the overall disease progression, reanalysis of such clinical trial data with regard to treatment effects on the macula-wide component of photoreceptor degeneration seems warranted.

Conclusions

In summary, this study outlines a fully automated pipeline to obtain photoreceptor degeneration related biomarkers in eyes with GA and provides accuracy estimates. A large between-eye variability in photoreceptor degeneration is evident, which is prognostic for future progression rates. Lastly, adjusting for age and retinal position (*z* score transformation) and accounting for the distance to the GA boundary, it is evident that outer retinal degeneration is a function of a junctional zone component, and an independent macula wide component over time. This framework could be used to detect beneficial treatment effects beyond mere GA lesion size progression.

ARTICLE INFORMATION

Accepted for Publication: June 28, 2020.

Published Online: August 13, 2020. doi:10.1001/jamaophthalmol.2020.2914

Author Contributions: Drs Pfau and Rubin had full access to all of the data in the study and take responsibility for the integrity of the data and the accuracy of the data analysis.
Concept and design: Pfau, von der Emde, de Sisternes, Leng, Schmitz-Valckenberg, Fleckenstein, Rubin.
Acquisition, analysis, or interpretation of data: Pfau, von der Emde, Hallak, Schmitz-Valckenberg, Holz, Fleckenstein, Rubin.
Drafting of the manuscript: Pfau, von der Emde, Rubin.

Critical revision of the manuscript for important intellectual content: Pfau, von der Emde, de Sisternes, Hallak, Leng, Schmitz-Valckenberg, Holz, Fleckenstein.
Statistical analysis: Pfau, Hallak.
Obtained funding: Pfau, Schmitz-Valckenberg, Fleckenstein.
Administrative, technical, or material support: von der Emde, Leng, Schmitz-Valckenberg, Fleckenstein, Rubin.
Supervision: Leng, Schmitz-Valckenberg, Holz, Fleckenstein, Rubin.

Conflict of Interest Disclosures: Dr Pfau reported funding from German Research Foundation PF950/1-1 and the Association of Rhine-Westphalian Ophthalmologists to during the conduct of the study and nonfinancial support from Heidelberg Engineering, Heidelberg, Germany outside the submitted work. Dr de Sisternes reported other support from Carl Zeiss Meditec Inc outside the submitted work. Dr Leng reported grants from Kodiak, Topcon, and Targeted Therapy Technologies; grants and personal fees from Genentech; and personal fees from Zeiss outside the submitted work. Dr Schmitz-Valckenberg reported grants from Acucela/Kubota Vision and Katairo; grants and personal fees from Alcon/Novartis, Allergan, Bayer, Roche/Genentech, and Bioeq/Formycon; grants, personal fees, and nonfinancial support from Carl Zeiss MediTec AG; grants and nonfinancial support from Centervue; personal fees from Galimedix and Oxurion; grants and nonfinancial support from Heidelberg Engineering; and nonfinancial support from Optos outside the submitted work. Dr Holz reported grants and personal fees from Heidelberg Engineering and Zeiss and grants from Centervue and Optos during the conduct of the study; grants and personal fees from Novartis, Bayer, Roche/Genentech, Geuder, Acucela, Apellis, Allergan, and Kanghong outside the submitted work; and personal fees from Pixium Vision and Lin Bioscience outside the submitted work. Dr Fleckenstein reported grants from German Research Foundation and personal fees and nonfinancial support from Heidelberg Engineering during the conduct of the study; nonfinancial support from Carl Zeiss Meditec and CenterVue; and grants and personal fees from Alcon/Novartis, Bayer, and Genentech/Roche outside the submitted work; in addition, Dr Fleckenstein had a patent to US20140303013A1 pending. Dr Rubin reported a patent to US Patent issued. The Department of Ophthalmology, University of Bonn, received technical support from Heidelberg Engineering, Heidelberg, Germany, Carl Zeiss Meditec, Jena, Germany, and Centervue, Padova, Italy. No other disclosures were reported.

Funding/Support: This work was supported by the German Research Foundation grant PF950/1-1 to MP and grant FL 658/4-1 and FL 658/4-2 to Dr Fleckenstein, and by the Association of Rhine-Westphalian Ophthalmologists, Recklinghausen.

Role of the Funder/Sponsor: The funding sources had no role in the design and conduct of the study; collection, management, analysis, and interpretation of the data; preparation, review, or approval of the manuscript; and decision to submit the manuscript for publication.

Disclaimer: The authors alone are responsible for the content and writing of the manuscript. The views expressed are those of the authors.

REFERENCES

1. Cheung LK, Eaton A. Age-related macular degeneration. *Pharmacotherapy*. 2013;33(8):838-855. doi:10.1002/phar.1264

2. Holz FG, Schmitz-Valckenberg S, Fleckenstein M. Recent developments in the treatment of age-related macular degeneration. *J Clin Invest*. 2014;124(4):1430-1438. doi:10.1172/JCI71029

3. Rasmussen A, Bloch SB, Fuchs J, et al. A 4-year longitudinal study of 555 patients treated with ranibizumab for neovascular age-related macular degeneration. *Ophthalmology*. 2013;120(12):2630-2636. doi:10.1016/j.ophtha.2013.05.018

4. Bakri SJ, Thorne JE, Ho AC, et al. Safety and efficacy of anti-vascular endothelial growth factor therapies for neovascular age-related macular degeneration: a report by the American Academy of Ophthalmology. *Ophthalmology*. 2019;126(1):55-63. doi:10.1016/j.ophtha.2018.07.028

5. Lindner M, Nadal J, Mauschitz MM, et al. Combined fundus autofluorescence and near infrared reflectance as prognostic biomarkers for visual acuity in foveal-sparing geographic atrophy. *Invest Ophthalmol Vis Sci*. 2017;58(6):BIO61-BIO67. doi:10.1167/iovs.16-21210

6. Chakravarthy U, Bailey CC, Johnston RL, et al. Characterizing disease burden and progression of geographic atrophy secondary to age-related macular degeneration. *Ophthalmology*. 2018;125(6):842-849. doi:10.1016/j.ophtha.2017.11.036

7. Sivaprasad S, Tschosik E, Kapre A, et al. Reliability and construct validity of the NEI VFQ-25 in a subset of patients with geographic atrophy from the phase 2 MAHALO study. *Am J Ophthalmol*. 2018;190:1-8. doi:10.1016/j.ajo.2018.03.006

8. Künzel SH, Möller PT, Lindner M, et al. Determinants of quality of life in geographic atrophy secondary to age-related macular degeneration. *Invest Ophthalmol Vis Sci*. 2020;61(5):63. doi:10.1167/iovs.61.5.63

9. Holz FG, Sadda SR, Busbee B, et al; Chroma and Spectri Study Investigators. Efficacy and safety of lampalizumab for geographic atrophy due to age-related macular degeneration: chroma and spectri phase 3 randomized clinical trials. *JAMA Ophthalmol*. 2018;136(6):666-677. doi:10.1001/jamaophthalmol.2018.1544

10. Spaide RF. Outer retinal atrophy after regression of subretinal drusenoid deposits as a newly recognized form of late age-related macular degeneration. *Retina*. 2013;33(9):1800-1808. doi:10.1097/IAE.0b013e31829c3765

11. Chen L, Messinger JD, Zhang Y, Spaide RF, Freund KB, Curcio CA. Subretinal drusenoid deposit in age-related macular degeneration: histologic insights into initiation, progression to atrophy, and imaging. *Retina*. 2020;40(4):618-631. doi:10.1097/IAE.0000000000002657

12. Steinberg JS, Saßmannshausen M, Fleckenstein M, et al. Correlation of partial outer retinal thickness with scotopic and mesopic fundus-controlled perimetry in patients with reticular drusen. *Am J Ophthalmol*. 2016;168:52-61. doi:10.1016/j.ajo.2016.04.025

13. Gin TJ, Wu Z, Chew SKH, Guymer RH, Luu CD. Quantitative analysis of the ellipsoid zone intensity in phenotypic variations of intermediate age-related macular degeneration. *Invest Ophthalmol Vis Sci*. 2017;58(4):2079-2086. doi:10.1167/iovs.16-20105

14. Pfau M, Lindner M, Gliem M, et al. Mesopic and dark-adapted two-color fundus-controlled perimetry in patients with cuticular, reticular, and soft drusen. *Eye (Lond)*. 2018;32(12):1819-1830. doi:10.1038/s41433-018-0183-3

15. Toth CA, Tai V, Pistilli M, et al; Comparison of Age-related Macular Degeneration Treatments Trials Research Group. Distribution of OCT features within areas of macular atrophy or scar after 2 years of anti-VEGF treatment for neovascular AMD in CATT. *Ophthalmol Retina*. 2019;3(4):316-325. doi:10.1016/j.oret.2018.11.011

16. Pfau M, Emde LV, Dysli C, et al. Determinants of cone- and rod-function in geographic atrophy: AI-based structure-function correlation. *Am J Ophthalmol*. 2020;S0002-9394(20)30170-7. doi:10.1016/j.ajo.2020.04.003

17. Sadda SR, Guymer R, Holz FG, et al. Consensus definition for atrophy associated with age-related macular degeneration on OCT: classification of atrophy report 3. *Ophthalmology*. 2018;125(4):537-548. doi:10.1016/j.ophtha.2017.09.028

18. Lindner M, Böker A, Mauschitz MM, et al; Fundus Autofluorescence in Age-Related Macular Degeneration Study Group. Directional kinetics of geographic atrophy progression in age-related macular degeneration with foveal sparing. *Ophthalmology*. 2015;122(7):1356-1365. doi:10.1016/j.ophtha.2015.03.027

19. Pfau M, Lindner M, Goerdt L, et al; Fundus Autofluorescence in Age-Related Macular Degeneration Study Group. Prognostic value of shape-descriptive factors for the progression of geographic atrophy secondary to age-related macular degeneration. *Retina*. 2019;39(8):1527-1540. doi:10.1097/IAE.0000000000002206

20. Pfau M, Möller PT, Künzel SH, et al. Type 1 choroidal neovascularization is associated with reduced localized progression of atrophy in age-related macular degeneration. *Ophthalmol Retina*. 2020;4(3):238-248. doi:10.1016/j.oret.2019.09.016

21. Fleckenstein M, Grassmann F, Lindner M, et al. Distinct genetic risk profile of the rapidly progressing diffuse-trickling subtype of geographic atrophy in age-related macular degeneration (AMD). *Invest Ophthalmol Vis Sci*. 2016;57(6):2463-2471. doi:10.1167/iovs.15-18593

22. Müller PL, Pfau M, Möller PT, et al. Choroidal flow signal in late-onset stargardt disease and age-related macular degeneration: An OCT-angiography study. *Invest Ophthalmol Vis Sci*. 2018;59(4):AMD122-AMD131. doi:10.1167/iovs.18-23819

23. von der Emde L, Pfau M, Dysli C, et al. Artificial intelligence for morphology-based function prediction in neovascular age-related macular degeneration. *Sci Rep*. 2019;9(1):11132. doi:10.1038/s41598-019-47565-y

24. Bates D, Mächler M, Bolker BM, Walker SC. Fitting linear mixed-effects models using lme4. *J Stat Softw*. 2015;67(1). doi:10.18637/jss.v067.i01

25. Groll A, Tutz G. Variable selection for generalized linear mixed models by L1-penalized estimation. *Stat Comput*. 2014;24(2):137-154. doi:10.1007/s11222-012-9359-z

26. Pfau M, Goerdt L, Schmitz-Valckenberg S, et al. Green-light autofluorescence versus combined blue-light autofluorescence and near-infrared

reflectance imaging in geographic atrophy secondary to age-related macular degeneration. *Invest Ophthalmol Vis Sci*. 2017;58(6):BIO121-BIO130. doi:10.1167/iovs.17-21764

27. Schmitz-Valckenberg S, Brinkmann CK, Alten F, et al. Semiautomated image processing method for identification and quantification of geographic atrophy in age-related macular degeneration. *Invest Ophthalmol Vis Sci*. 2011;52(10):7640-7646. doi:10.1167/iovs.11-7457

28. Niu S, Chen Q, de Sisternes L, Rubin DL, Zhang W, Liu Q. Automated retinal layers segmentation in SD-OCT images using dual-gradient and spatial correlation smoothness constraint. *Comput Biol Med*. 2014;54:116-128. doi:10.1016/j.compbiomed.2014.08.028

29. Gorgi Zadeh S, Wintergerst MWM, Wiens V, et al CNNs enable accurate and fast segmentation of drusen in optical coherence tomography. In: Cardoso MJ, Arbel T, Carneiro G, et al., eds. *Lecture Notes in Computer Science (Including Subseries Lecture Notes in Artificial Intelligence and Lecture Notes in Bioinformatics)*. Springer International Publishing; 2017:65-73.

30. Fang L, Cunefare D, Wang C, Guymer RH, Li S, Farsiu S. Automatic segmentation of nine retinal layer boundaries in OCT images of non-exudative AMD patients using deep learning and graph search. *Biomed Opt Express*. 2017;8(5):2732-2744. doi:10.1364/BOE.8.002732

31. Maloca PM, Lee AY, de Carvalho ER, et al. Validation of automated artificial intelligence segmentation of optical coherence tomography images. *PLoS One*. 2019;14(8):e0220063. doi:10.1371/journal.pone.0220063

32. Holz FG, Bindewald-Wittich A, Fleckenstein M, Dreyhaupt J, Scholl HPN, Schmitz-Valckenberg S; FAM-Study Group. Progression of geographic atrophy and impact of fundus autofluorescence patterns in age-related macular degeneration. *Am J Ophthalmol*. 2007;143(3):463-472. doi:10.1016/j.ajo.2006.11.041

33. Domalpally A, Danis RP, White J, et al. Circularity index as a risk factor for progression of geographic atrophy. *Ophthalmology*. 2013;120(12):2666-2671. doi:10.1016/j.ophtha.2013.07.047

34. Lindner M, Kosanetzky S, Pfau M, et al; FAM-Study Group. Local progression kinetics of geographic atrophy in age-related macular degeneration are associated with atrophy border morphology. *Invest Ophthalmol Vis Sci*. 2018;59(4):AMD12-AMD18. doi:10.1167/iovs.17-23203

35. Nassisi M, Baghdasaryan E, Borrelli E, Ip M, Sadda SR. Choriocapillaris flow impairment surrounding geographic atrophy correlates with disease progression. *PLoS One*. 2019;14(2):e0212563-e0212563. doi:10.1371/journal.pone.0212563

36. Thulliez M, Zhang Q, Shi Y, et al. Correlations between choriocapillaris flow deficits around geographic atrophy and enlargement rates based on swept-source OCT imaging. *Ophthalmol Retina*. 2019;3(6):478-488. doi:10.1016/j.oret.2019.01.024

37. Nunes RP, Gregori G, Yehoshua Z, et al. Predicting the progression of geographic atrophy in age-related macular degeneration with SD-OCT en face imaging of the outer retina. *Ophthalmic Surg Lasers Imaging Retina*. 2013;44(4):344-359. doi:10.3928/23258160-20130715-06

38. Domalpally A, Agrón E, Pak JW, et al. Prevalence, risk, and genetic association of reticular pseudodrusen in age-related macular degeneration: age-related eye disease study 2 report 21. *Ophthalmology*. 2019;126(12):1659-1666. doi:10.1016/j.ophtha.2019.07.022

39. Neely D, Zarubina AV, Clark ME, et al. Association between visual function and subretinal drusenoid deposits in normal and early age-related macular degeneration eyes. *Retina*. 2017;37(7):1329-1336. doi:10.1097/IAE.0000000000001454

40. Spaide RF, Ooto S, Curcio CA. Subretinal drusenoid deposits AKA pseudodrusen. *Surv Ophthalmol*. 2018;63(6):782-815. doi:10.1016/j.survophthal.2018.05.005

41. Zhang Y, Wang X, Sadda SR, et al. Lifecycles of individual subretinal drusenoid deposits and evolution of outer retinal atrophy in age-related macular degeneration. *Ophthalmol Retina*. 2020;4(3):274-283. doi:10.1016/j.oret.2019.10.012

42. Takahashi A, Ooto S, Yamashiro K, et al. Photoreceptor damage and reduction of retinal sensitivity surrounding geographic atrophy in age-related macular degeneration. *Am J Ophthalmol*. 2016;168:260-268. doi:10.1016/j.ajo.2016.06.006

43. Pfau M, von der Emde L, Dysli C, et al. Light sensitivity within areas of geographic atrophy secondary to age-related macular degeneration. *Invest Ophthalmol Vis Sci*. 2019;60(12):3992-4001. doi:10.1167/iovs.19-27178

44. Pfau M, Müller PL, von der Emde L, et al. Mesopic and dark-adapted two-color fundus-controlled perimetry in geographic atrophy secondary to age-related macular degeneration. *Retina*. 2020;40(1):169-180. doi:10.1097/IAE.0000000000002337

45. Owsley C, McGwin G Jr, Jackson GR, Kallies K, Clark M. Cone- and rod-mediated dark adaptation impairment in age-related maculopathy. *Ophthalmology*. 2007;114(9):1728-1735. doi:10.1016/j.ophtha.2006.12.023

46. Moult EM, Alibhai AY, Lee B, et al. A framework for multiscale quantitation of relationships between choriocapillaris flow impairment and geographic atrophy growth. *Am J Ophthalmol*. 2020;214(January):172-187. doi:10.1016/j.ajo.2019.12.006

47. Li M, Huisingh C, Messinger J, et al. Histology of geographic atrophy secondary to age-related macular degeneration a multilayer approach. *Retina*. 2018;38(10):1937-1953. doi:10.1097/IAE.0000000000002182

48. Zanzottera EC, Ach T, Huisingh C, Messinger JD, Freund KB, Curcio CA. Visualizing retinal pigment epithelium phenotypes in the transition to atrophy in neovascular age-related macular degeneration. *Retina*. 2016;36(suppl 1):S26-S39. doi:10.1097/IAE.0000000000001330

49. Dolz-Marco R, Balaratnasingam C, Messinger JD, et al. The border of macular atrophy in age-related macular degeneration: a clinicopathologic correlation. *Am J Ophthalmol*. 2018;193:166-177. doi:10.1016/j.ajo.2018.06.020

50. Niu S, de Sisternes L, Chen Q, Rubin DL, Leng T. Fully automated prediction of geographic atrophy growth using quantitative spectral-domain optical coherence tomography biomarkers. *Ophthalmology*. 2016;123(8):1737-1750. doi:10.1016/j.ophtha.2016.04.042

51. Lu CD, Lee B, Schottenhamml J, Maier A, Pugh EN Jr, Fujimoto JG. Photoreceptor layer thickness changes during dark adaptation observed with ultrahigh-resolution optical coherence tomography. *Invest Ophthalmol Vis Sci*. 2017;58(11):4632-4643. doi:10.1167/iovs.17-22171

52. Curcio CA. Soft drusen in age-related macular degeneration: Biology and targeting via the oil spill strategies. *Invest Ophthalmol Vis Sci*. 2018;59(4):AMD160-AMD181. doi:10.1167/iovs.18-24882